SELF-EXCITATION CONDITIONS FOR A LABORATORY MODEL OF A GEOMAGNETIC DYNAMO

A. Gailitis

Magnitnaya Gidrodinamika, Vol. 3, No. 3, pp. 45–54, 1967

UDC 538.4

The author examines a laboratory model of a geomagnetic dynamo consisting of a hollow sphere with a certain internal small-scale organization of liquid metal flow. The self-excitation conditions are established by solving the electrodynamic equations averaged over the small-scale motion. The magnetic field and current distributions are given.

The origin of the magnetic field of the earth, the other planets, the sun, and the stars is currently explained in terms of its generation in the convective regions of these bodies. According to Steenbeck, Krause, and Rädler [1–6], an important part in this process is played by the gyrotropicity* of turbulence due to rotation, which in conducting fluids creates an emf along the mean magnetic field and hence, in principle, can produce self-excitation.

In order to test this hypothesis Steenbeck [6] has proposed the construction of a laboratory model. The present article is concerned with a certain modification of that model proposed by I. Kirko, in which the gyrotropic turbulence is simulated by means of a certain pseudo-turbulent motion.

1. Schematic description of the model. The proposed model consists of a cube divided by electrically conducting walls into 12 × 12 parallel channels of square ($l \times l$) cross section. Outside the cube neighboring channels are connected to form a continuous hydraulic circuit through which liquid sodium is pumped by an external pump. The channels are assumed to be so connected that in any two neighboring (separated by a wall) channels the sodium flows in opposite directions. Helical guides of the same helicity (i.e., all right-handed or all left-handed) are built into the elements connecting neighboring channels with the object of forcing the sodium to rotate about the channel axis, as well as undergo translational motion.

In order to facilitate the magnetic field self-excitation calculations, the model is simplified in two respects. First, it is assumed that there are not 12 × 12 but considerably more, in the limit an infinitely large number of channels. In the next section of this paper the averaged electrodynamic characteristics of small sections of the model are determined on this basis. The self-excitation conditions are found by solving the averaged electrodynamic equations. In this case a second assumption is made, namely, that the cube is replaced by a spherical volume of the same structure as the cube (Fig. 1). The problem of the excitation of such a volume is solved in the third section.**

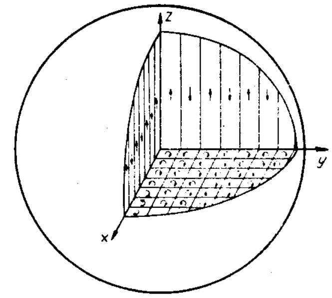

Fig. 1. Calculation model.

If the thickness of the walls is negligible, then, disregarding turbulent and viscous dissipation, we may assume that the velocity v_z*** is distributed according to the law

$$v_z = VS(x/l, y/l), \tag{1}$$

where

$$S(x, y) = s(x)s(y), \tag{2}$$

and s(x) is a periodic, piecewise-constant function taking the two values ±1 (Fig. 2). Below we employ the Fourier expansions of these functions,

$$s(x) = \frac{2}{\pi}\sum_{k=-\infty}^{\infty}\frac{(-1)^k}{(2k+1)}e^{(2k+1)i\pi x}, \tag{3}$$

$$S(x, y) = \frac{4}{\pi^2}\sum_{k,l=-\infty}^{+\infty}\frac{(-1)^{k+l}}{(2k+1)(2l+1)}e^{(2k+1)i\pi x+(2l+1)i\pi y}. \tag{4}$$

If the sodium rotates in the helical guides as a solid and the inlet to the channels is made sufficiently smooth, the rotation will continue in the channels also, $\mathrm{rot}_z\,\mathbf{v}$ being proportional to v_z,

$$\mathrm{rot}_z\,\mathbf{v} = \Omega S(x/l, y/l). \tag{5}$$

*Correlation between turbulent velocity **v** and rot **v**, i.e., preponderance of right-handed over left-handed motions or vice versa.

**The estimate obtained in [7] is for an infinite cylinder.

***The z axis is directed along the channels, the x, y axes parallel to the walls.

Expression (5) differs from (1) with respect to the coefficient Ω, which is expressed below [see (13)] in terms of the root mean square rate of rotation *

$$v_\perp = (\overline{v_x^2} + \overline{v_y^2})^{1/2}. \qquad (6)$$

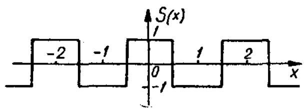

Fig. 2. Determination of the function s(x).

Since

$$\text{rot rot } \mathbf{v} = \text{grad div } \mathbf{v} - \Delta\mathbf{v}, \qquad (7)$$

and by virtue of the incompressibility

$$\text{div } \mathbf{v} = 0, \qquad (8)$$

we have

$$\mathbf{v} = (-\Delta)^{-1} \text{ rot rot } \mathbf{v} \qquad (9)$$

or

$$v_x = \Omega \frac{\partial}{\partial y}(-\Delta)^{-1} S(x/l, y/l), \qquad (10)$$

$$v_y = -\Omega \frac{\partial}{\partial x}(-\Delta)^{-1} S(x/l, y/l). \qquad (11)$$

Here, $(\Delta)^{-1}$ is the inverse Laplace operator, which acts on the function (4) according to the law

$$(-\Delta)^{-1} S(x, y) = \frac{4}{\pi^2} \times$$
$$\times \sum_{k, n=-\infty}^{+\infty} \frac{(-1)^{k+n} e^{(2k+1)i\pi x + (2n+1)i\pi y}}{(2k+1)(2n+1)[(2k+1)^2 + (2n+1)^2]}. \qquad (12)$$

By means of (6), (10), (11), and (12) it is easy to obtain

$$\Omega^2 = v_\perp^2 \gamma_1^{-1} l^{-2}, \qquad (13)$$

where

$$\gamma_1 = \frac{64}{\pi^4} \sum_{k, n=0}^{\infty} (2k+1)^{-2} (2n+1)^{-2} [(2k+1)^2 +$$
$$+ (2n+1)^2]^{-1} = 0.3469\ldots. \qquad (14)$$

2. Averaged electromagnetic properties of model. In order to study self-excitation for a large number of channels it is most convenient to use the Maxwell equations for quantities averaged over the periodic structure of the model (i.e., over a distance $\sim l$). In this case the equations

$$\text{rot } \mathbf{H} = \mathbf{j}, \qquad (15)$$

$$\text{div } \mathbf{B} = 0 \qquad (16)$$

*The bar denotes averaging with respect to x, y.

for the averaged quantities are the same as for the local quantities. The only problem is averaging Ohm's law

$$\mathbf{j} = \sigma\{-\text{grad } \Phi + \mu[\mathbf{v} \times \mathbf{H}]\} \qquad (17)$$

(Φ is the electrostatic potential).

As the investigation is confined to the determination of the self-excitation conditions, motion (1), (10), (11) may be assumed independent of H. Therefore the result of averaging will linearly depend on the averaged field $\overline{\mathrm{H}}$ and its spatial derivatives. Confining ourselves to the first derivatives, from which it is possible to construct only one vector rot $\overline{\mathrm{H}}$, we have [4]

$$j_z = \sigma\{-\text{grad}_z \overline{\Phi} - \beta'_z \text{ rot}_z \overline{\mathbf{H}}\}, \qquad (18)$$

$$\mathbf{j}_\perp = \sigma\{-\text{grad}_\perp \overline{\Phi} - \beta'_\perp \text{ rot}_\perp \overline{\mathbf{H}} + \alpha' \overline{\mathbf{H}}_\perp\}. \qquad (19)*$$

In this model the direction of the z axis is not equivalent to the direction of the x and y axes, therefore, generally speaking, β'_z and $\beta'_\perp$ are different. Motion in a straight line along a uniform field and rotation about it do not create induction currents; therefore the term $\alpha'_z \overline{H}_z$ does not appear in (17).

In order to determine the constants α', β'_z, $\beta'_\perp$ it is necessary to represent the actual field H as the sum of the averaged field $h^{(0)} = \overline{H}(x, y, z)$ and a series of local perturbations $h^{(t)}$,

$$\mathbf{H} = \sum_{t=0}^{\infty} \mathbf{h}^{(t)}. \qquad (20)$$

Table 1

n	$d_n \times 10^{2n}$	X	n	$d_n \times 10^{2n}$	X
0	2.5	—	8	−0.23648	8.401
1	−5	7.071	9	−0.22844	8.357
2	1.30385	7.688	10	−0.13642	8.341
3	0.40274	7.868	11	−0.02384	8.339
4	0.67788	8.163	12	0.05959	8.343
5	0.43836	8.442	13	0.09210	8.346
6	0.14023	8.612	14	0.07861	8.348
7	−0.11284	8.495	15	0.03986	8.349
			16	−0.00087	8.349

Substitution of (20) into (15)–(17) gives the system of equations

$$\mathbf{h}^{(t)} = \mu\sigma \text{ rot } (-\Delta)^{-1} [\mathbf{v} \times \mathbf{h}^{(t-1)}] \qquad (21)$$

expressing the $h^{(t)}$ in terms of $h^{(t-1)}$ and, in the last analysis, all of them in terms of $h^{(0)} = \overline{H}$. The solution of (21) in accordance with (17) gives (18), (19) with the constants

$$\alpha' = 2\gamma_1^{1/2} \sigma^{-1} l^{-1} R_{mv} R_{m\perp} \left(1 + 0(R_{m\perp}^2)\right), \qquad (22)$$

$$\beta'_\perp = \gamma_1 \sigma^{-1} R_{mv}^2 \left(1 + 0(R_{m\perp}^2)\right). \qquad (23)$$

*The sign $\perp$ associated with a vector denotes its component in the plane (x, y).

Table 2

Field at center r = z = 0	H_0
Field at pole r = 0; z = R	$0.0415 H_0$
Maximum H_φ	$0.419\ H_0$
Maximum j_φ	$3.50\ H_0/R$
Maximum j_z	$2.65\ H_0/R$
Field outside sphere $\rho=(r^2+z^2)^{1/2}>1$. $s=z/\rho$	$\mathbf{H}=-\mathrm{grad}\,(0.0708\rho^{-2}P_1(s)-0.0306\rho^{-4}P_3(s)+0.0049\rho^{-6}P_5(s)-0.0003\rho^{-8}P_7(s)+\ldots)\times\mathbf{H}_0$

$$\beta'_z=\gamma_2\sigma^{-1}\gamma_1^{-1}R_{m\perp}^2\Big(1+0(R_{m\perp}^2)\Big), \tag{24}$$

where

$$\gamma_2=\frac{64}{\pi^4}\sum_{l,k=0}^{\infty}(2l+1)^{-2}[(2k+1)^2+$$
$$+(2l+1)^2]^{-3}=0.08292\ldots \tag{25}$$

[for γ_1 see (14)] and

$$R_{mV}=\mu\sigma Vl, \tag{26}$$

$$R_{m\perp}=\mu\sigma v_\perp l. \tag{27}$$

Substituting (22)–(24) into (18), (19), we obtain

$$\overline{j_z}=-\sigma_z\frac{\partial}{\partial z}\overline{\Phi}, \tag{28}$$

$$\overline{\mathbf{j}_\perp}=-\sigma_\perp\,\mathrm{grad}_\perp\overline{\Phi}+\alpha\overline{\mathbf{H}}_\perp, \tag{29}$$

where

$$\sigma_z=\sigma/(1+R_{m\perp}^2\gamma_2/\gamma_1), \tag{30}$$

$$\sigma_\perp=\sigma/(1+R_{mV}^2\gamma_1), \tag{31}$$

$$\alpha=2\gamma_1^{1/2}l^{-1}R_{mV}R_{m\perp}(1+\gamma_1R_{mV}^2)^{-1}. \tag{32}$$

3. Self-excitation conditions. The sodium velocity at which self-excitation occurs can be found by solving the system*

$$\mathrm{rot}_\perp\,\mathbf{H}=-\sigma_\perp\,\mathrm{grad}_\perp\,\Phi+\alpha\mathbf{H}_\perp;\quad \mathrm{rot}_z\,\mathbf{H}=-\sigma_z\,\mathrm{grad}_z\,\Phi;$$
$$\mathrm{div}\,\mathbf{H}=0 \tag{33}$$

for the eigenvalue, i.e., by determining the α (depending on $\sigma_z/\sigma_\perp$) for which (33) has a solution that on the boundary of the model (sphere of radius R) goes over continuously to the solution, decreasing to infinity, of the system

$$\mathrm{rot}\,\mathbf{H}=0,\qquad \mathrm{div}\,\mathbf{H}=0. \tag{34}$$

Self-excitation is possible at velocities for which expression (32) is equal to or greater than the least eigenvalue of the system (33), (34).

If we replace α in (33) with the dimensionless quantity

$$X=\alpha R, \tag{35}$$

we can reduce the problem to solution of system (33) within the unit sphere and system (34) outside it.

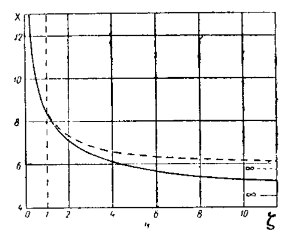

Fig. 3. Least root of Eq. (54) as a function of ζ.

Below we will consider only axisymmetric solutions of (33), (34). Then, in cylindrical coordinates ($r=(x^2+y^2)^{1/2}$, z) (33) assumes the form

$$\frac{1}{r}\frac{\partial}{\partial r}rH_r=-\frac{\partial H_z}{\partial z},\quad \frac{\partial H_z}{\partial r}=\frac{\partial H_r}{\partial z}-XH_\varphi,$$
$$\frac{1}{r}\frac{\partial}{\partial r}rH_\varphi=-\zeta\frac{\partial\psi}{\partial z},\quad \frac{\partial\psi}{\partial r}=\frac{\partial H_\varphi}{\partial z}+XH_r, \tag{36}$$

where

$$\zeta=\sigma_z/\sigma_\perp, \tag{37}$$

$$\psi=\sigma_\perp\Phi. \tag{38}$$

It is convenient to find the solution of (36) in series form,

$$H_r=\sum_{k,l,j}a^k_{l,j}r^{2j+1}z^{l-2j-1}X^k,$$
$$H_\varphi=\sum_{k,l,j}b^k_{l,j}r^{2j+1}z^{l-2j-1}X^k,$$
$$H_z=\sum_{k,l,j}c^k_{l,j}r^{2j}z^{l-2j}X^k,\quad \psi=\sum_{k,l,j}f^k_{l,j}r^{2j}z^{l-2j}X^k. \tag{39}$$

In accordance with (36) the coefficients $a^k_{l,j}$, $b^k_{l,j}$, $c^k_{l,j}$, $f^k_{l,j}$ (except $c^k_{l,0}$ and $f^k_{l,0}$) are given by the recurrence relations

$$a^k_{l,j}=-(l-2j)c^k_{l,j}(2j+2)^{-1},$$
$$c^k_{l,j+1}=\Big((l-2j-1)a^k_{l,j}-b^{k-1}_{l-1,j}\Big)(2j+2)^{-1},$$
$$b^k_{l,j}=-\zeta(l-2j)f^k_{l,j}(2j+2)^{-1}.$$
$$f^k_{l,j}=\Big((l-2j-1)b^k_{l,j}+a^{k-1}_{l-1,j}\Big)(2j+2)^{-1}. \tag{40}$$

The coefficients $c^k_{l,0}$ and $f^k_{l,0}$ are not found from system (40) and must be selected so that on the surface

*In what follows only averaged quantities are used and to simplify the equations the averaging bar has been dropped.

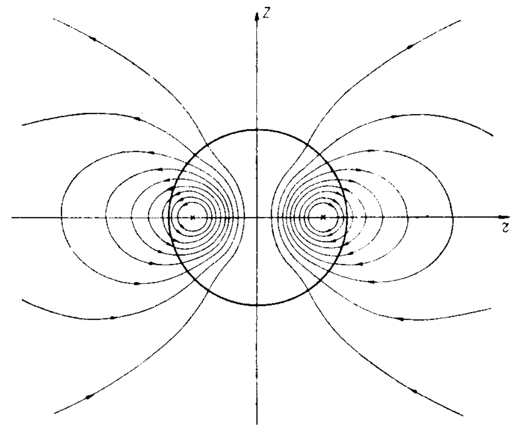

Fig. 4. Magnetic field lines for the r, z components.

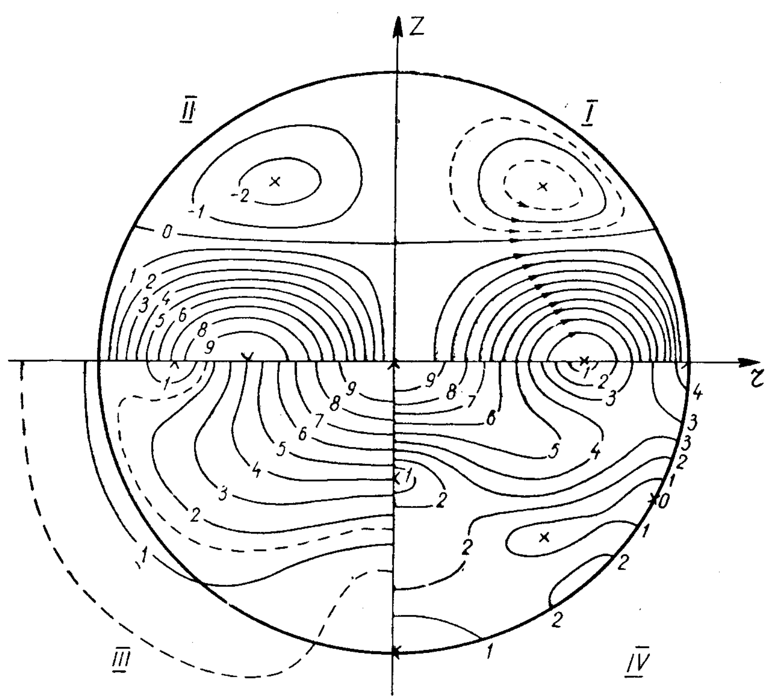

Fig. 5. Quadrant I — directions of the r, z current components. Quadrant II — level lines of azimuthal field H_φ and current j_φ. Quadrant III — level lines $(H_r^2 + H_z^2)^{1/2}$. Quadrant IV — level lines $(j_r^2 + j_z^2)^{1/2}$. Solid curves — principal level lines at intervals of 1/10 maximum value of the given quantity, direction lines at intervals of 1/10 the corresponding stream function. The lines are numbered in order of increase in magnitude. Dashed curves — half-level lines. ×— extremal points.

$r^2 + z^2 = 1$ solution (39) goes over continuously into the solution of system (34). When $r^2 + z^2 > 1$ the latter takes the form

$$\mathbf{H} = -\operatorname{grad}\tau, \tag{41}$$

where

$$\tau = \sum_{n=1}^{\infty} D_n (n+1)^{-1} (r^2+z^2)^{-(n+1)/2} P_n\left(z/(r^2+z^2)^{1/2}\right). \tag{42}$$

when $r^2 + z^2 = 1$ Eqs. (39) behave as sums of polynomials in powers of z,

$$H_r/r = \sum_{k,l,j} a^k_{l,j}(1-z^2)^j z^{l-2j-1} X^k,$$

$$H_\varphi/r = \sum_{k,l,j} b^k_{l,j}(1-z^2)^j z^{l-2j-1} X^k,$$

$$H_z = \sum_{k,l,j} c^k_{l,j}(1-z^2)^j z^{l-2j} X^k, \tag{43}$$

and (42) as a sum of Legendre polynomials $P_n(z)$ and their derivatives

$$H_r/r = \sum_n D_n\left(1 + \frac{z}{(n+1)}\frac{d}{dz}\right)P_n(z), \tag{44}$$

$$H_\varphi = 0, \tag{45}$$

$$H_z = \sum_n D_n P_{n+1}(z). \tag{46}$$

The sums in (43) can be written in a form analogous to (44)–(46),

$$\sum_{l,j} a^k_{l,j}(1-z^2)^j z^{l-2j-1} = \sum_n d^k_{rn}\left(1 + \frac{z}{n+1}\frac{d}{dz}\right)P_n(z), \tag{47}$$

$$\sum_{l,j} b^k_{l,j}(1-z^2)^j z^{l-2j-1} = \sum_t g^k_t z^t, \tag{48}$$

$$\sum_{l,j} c^k_{l,j}(1-z^2)^j z^{l-2j} = \sum_n d^k_{zn} P_{n+1}(z). \tag{49}$$

If $a^k_{l,j}$, $b^k_{l,j}$, and $c^k_{l,j}$ are known, it is easy to compute the corresponding coefficients d^k_{rn}, g^k_t and d^k_{zn} by means of Newton's binomial and the formulas of the theory of Legendre polynomials. The coefficients $c^k_{l,0}$ and $f^k_{l,0}$ must be selected so that the magnetic field changes continuously on the unit sphere, i.e., so that at $r^2 + z^2 = 1$ solutions (43) coincide with (44)–(46), in other words, at any n and t

$$\sum_k d^k_{rn} X^k = \sum_k d^k_{zn} X^k, \qquad \sum_k g^k_t X^k = 0. \tag{50}$$

Equations (50) do not determine the coefficients $c^k_{l,0}$ and $f^k_{l,0}$ uniquely, which makes it possible to impose additional conditions*

$$g^k_t = 0 \text{ and } d^k_{rn} = d^k_{zn} \tag{51}$$

for $n \neq 2$ and all k and t. Then all Eqs. (50) except one (n = 2) are automatically satisfied. The latter is the equation for the eigenvalue X.

The selection of $c^k_{l,0}$, $f^k_{l,0}$ and the determination of the coefficients of this equation were programmed for a computer and executed in the following sequence.

1. Since (51) admits an arbitrary choice of $c^k_{2,0}$, the latter were assigned as follows:

$$c^k_{2,0} = \delta_{k0} = \begin{cases} 1, & k=0, \\ 0, & k \neq 0. \end{cases} \tag{52}$$

2. The remaining $c^k_{l,0}$ and $f^k_{l,0}$ were selected so that conditions (51) were satisfied. The selection procedure is facilitated in that with (52) all the $a^k_{l,j} = b^k_{l,j} = c^k_{l,j} = f^k_{l,j} = 0$, provided that $l > k + 2$, and in that for a given k only d^k_{rn}, d^k_{zn} with $n \leq l$ depends on the quantity $c^k_{l,0}$ and only g^k_t with $t \leq l$ on $f^k_{l,0}$. This made it possible to perform the selection sequentially with respect to one coefficient: $c^k_{k+2,0}$ was found from the condition $d^k_{rk+2} = d^k_{zk+2}$, $c^k_{k,0}$ from $d^k_{rk} = d^k_{zk}$, ... $c^k_{l,0}$ from $d^k_{rl} = d^k_{zl}$..., and so on for all $l \neq 2$ from k + 2 to 0. Then $f^k_{l,0}$ was similarly determined from $g^k_l = 0$.

For the purposes of a numerical selection the quantity $c^k_{l,0}$ (and similarly $f^k_{l,0}$) was given two arbitrary numerical values, for both of which we computed from (40) all the $a^k_{l,j}$, $c^k_{l,j}$ and the corresponding d^k_{rl} and d^k_{zl}. Then, by linear interpolation we found the value of $c^k_{l,0}$ that satisfies (51). Owing to the linearity of our equations, linear interpolation gives the "true" value of $c^k_{l,0}$. For the latter we determined the "true" values of $a^k_{l,j}$ and $c^k_{l,j}$, which were used in the subsequent selection steps. Selection began at k = 0, when it is necessary to select only one coefficient $c^0_{0,0}$ (since $c^0_{2,0}$ is given at the beginning of the calculations by (52)), continued at k = 1, when likewise only $f^1_{1,0}$ was determined, at k = 2, when there were two $c^2_{4,0}, c^2_{0,0}$ and so on, i.e., for each even k we successively selected all $c^k_{l,0}$ with $l \neq 2$ from k + 2 to 0, then increased k by one and selected all the $f^k_{l,0}$ with l from k to 1, then again increased k by one and selected the $c^k_{l,0}$, and so on until the necessary number of coefficients had been found.

Since $c^k_{2,0}$ is given from the beginning, it is not possible to make the differences $(d^k_{r2} - d^k_{z2})$ vanish in the way indicated above. Instead the calculations give certain numerical values. Therefore boundary conditions (50) are satisfied if X is a root of the equation

$$\sum_{k=0}^{\infty} (d^k_{r2} - d^k_{z2}) X^k = 0. \tag{53}$$

In fact, (53) contains only even powers of X, i.e., has the form

$$\sum_{n=0}^{\infty} d_n X^{2n} = 0. \tag{54}$$

The first coefficients of Eq. (54), computed for $\zeta = 1$, are in the second column of Table 1 (p. 24). The

*Conditions (51) lead to a solution with a certain symmetry. On obtaining a solution with another symmetry see below.

third column contains the least real root obtained by numerical solution of Eq. (54) neglecting terms of degree higher than 2n. As may be seen from the table, the convergence of the calculation is quite satisfactory, and cutting off infinite series (54) after the first eleven terms gives more than enough accuracy for our purposes.

It should be noted that in the solution obtained H_z and ψ are even functions of z, while H_r and H_φ are odd,

$$H_z(-z,r)=H_z(z,r),\quad \psi(-z,r)=\psi(z,r),$$

$$H_r(-z,r)=-H_r(z,r),\quad H_\varphi(-z,r)=-H_\varphi(z,r). \quad (55)$$

There is also a second type of solution in which H_r, H_φ are even and H_z, ψ odd functions of z. This solution, which henceforth we shall call the odd solution, was found with a certain modification in the procedure described above. For this it was required to satisfy conditions (51) for all $n \neq 3$, while assigning the coefficient $c^k{}_{3,0} = \delta_{k0}$, and not $c^k{}_{2,0}$ as in (52) for the even solution.

Equation (54), cut off after eleven terms, was solved for a series of values of $\zeta = \sigma_z/\sigma_\perp$; the dependence of the least root X on ζ is presented in Fig. 3, the solid curve corresponding to the even, the dashed curve to the odd solution. At large ζ the values of X tend to the constant limits 4.493 and 5.763 for the even and odd solutions, respectively. At $\zeta = 1$ the two curves intersect, but their difference at $\zeta < 1$ is so slight that in Fig. 3 it is not possible to show them as separate lines. At $\zeta \ll 1$ the values of X increase as $\sim\zeta^{-1/2}$.

In addition, we calculated the magnetic field and electric current distribution for the even solution at $\zeta = 1$. Certain numerical values are presented in Table 2; the magnetic field lines, the electric current flow lines and the field and current level lines are represented in Figs. 4 and 5.

It is clear from Table 2 that the field outside the sphere is the sum of the dipole and octupole fields with a small contribution from the higher multipoles. The large value of the octupole term is associated with the presence in the system of three current "vortices" (see quadrants I and II in Fig. 5). The chief of these occupies the equatorial region ($|z| \leqslant 0.4$), the two secondary ones the polar regions. The direction of the currents in the secondary "vortices" is opposite to that in the principal "vortex."

In each current "vortex" the central current flow line is a circle with center on the z axis. The other lines are spirals winding around this circle. After a large number of revolutions each current flow line covers a hill-like surface about the z axis. The magnetic field lines behave similarly, but they all belong to a single "vortex."

4. Optimal size of model. In accordance with (32), (35), the beginning of self-excitation is determined by the condition

$$R_m^2 \equiv \frac{R_{mV} R_{m\perp}}{1+0.347 R_{mV}^2}\,\frac{R}{l} = 0.86 X(\zeta). \quad (56)$$

At $\zeta = 1$ the right side of (56) takes the value 7.15 and close to $\zeta = 1$ depends relatively weakly on its argument

$$\zeta = (1+0.347 R_{mV}^2)/(1+0.24 R_{m\perp}^2). \quad (57)$$

However, in accordance with (26) and (27), at small R_{mV} the left side is the square of the effective magnetic Reynolds number, in whose construction the geometric mean of l and R is taken as the linear dimension and the geometric mean of V and $v_\perp$ as the velocity. If in (56) we neglect the dependence of X on ζ, then for liquid sodium at 100° C

$$v_\perp VRl/(1+0.347 R_{mV}^2) = 0.0416\ \mathrm{m^4/sec^2}. \quad (58)$$

In order to obtain satisfaction of (58) for a moderate total kinetic energy V and $v_\perp$ must be comparable quantities. With the given construction it is technically more difficult to increase $v_\perp$ than V, and $R_{m\perp}$ will always be less than R_{mV}. If it is not possible to obtain a sufficient rate of rotation, increasing V alone is insufficient, since this leads to an increase in the denominator. Making the channels too fine is also impermissible. The optimum value of l in accordance with (58) is determined by equality of its denominator to 2. Estimate (58) was obtained by neglecting the dependence of X on ζ. Taking the latter into account graphically at $R_{m\perp}$ less than R_{mV} increases the optimal value of the denominator to 2.8, which corresponds to

$$l = 2.3/\mu\sigma V, \quad (59)$$

$$v_\perp VRl = 1.6\mu^{-2}\sigma^{-2} = 0.092\ \mathrm{m^4/sec^2}\,\Big|_{\mathrm{Na}\ 100^\circ \mathrm{C}}. \quad (60)$$

Estimates (59), (60), like the entire argument, presuppose $l \ll$ R and tell nothing about the situation when $l \sim$ R.

The current distribution (see Fig. 5) and the almost identical conditions of excitation of both types of field show that the spherical shape is not optimal. Clearly, a preferable model is one in the form of a short cylinder of roughly equal height and radius, since elimination of the polar current "vortices" leads to savings without serious loss of intensity.

The center of the system, where no induction emf is created and only the electric currents close, is also a passive region of the model. Here, in order to reduce resistance losses it is desirable to replace the channels with copper bars with a conductivity higher than that of sodium.

REFERENCES

1. M. Steenbeck, Monatsber. Dtsch. Akad. Wiss. Berlin, 5, 625, 1963.

2. F. Krause, Czechosl. Acad. Sc. Astron. Inst., publication no. 51, 32, 1963.

---

*These values are the least nonzero roots of the Bessel functions $J_{3/2}(X)$ and $J_{5/2}(X)$.

3. F. Krause, Stellar and Solar Magnetic Fields. Amsterdam, ed. R. Lüst, North Holland Publishing Co., 426, 1965.
4. M. Steenbeck, F. Krause and K.H. Rädler, Z.f. Naturf., 21a, 369, 1966.
5. M. Steenbeck and F. Krause, Z.f. Naturf., 21a, 1285, 1966.
6. M. Steenbeck and F. Krause, Magnitnaya gidrodinamika [Magnetohydrodynamics], 3, 19, 1967.
7. F. Krause, Z.f. Naturf. (in press).

4 February 1967